Published by :
https://www.ijert.org/
An International Peer-Reviewed Journal

International Journal of Engineering Research & Technology (IJERT)
ISSN: 2278-0181
Vol. 15 Issue 06 , June - 2026

Exchange-Driven Sodium Hazard During Coastal Aquifer Freshening: Implications for Irrigation Water Quality in Paravur, India

Mophin Kani K*
Dept of Civil Engineering (Environmental Engineering and Management), UKF College of Engineering and Technology, Parippally, Kollam 691302, Kerala, India

Abstract **-** Coastal subsurface groundwater frequently experiences seawater intrusion, affecting groundwater suitability for irrigation. This study evaluates irrigation water quality in the Paravur coastal aquifer, Kerala, India, with emphasis on sodium hazards associated with salinisation processes. A total of 100 groundwater samples were collected along a 9-km coastal–inland transect during the 2025 dry season. Hydrochemical facies, ionic ratios (Cl/Na and the chlorinity index), Base Exchange Index (BEX), principal component analysis (PCA), and irrigation suitability indices, including Kelly's Ratio (KR), Magnesium Hazard (MH), Permeability Index (PI), and Residual Sodium Carbonate (RSC), were applied. Results reveal an unexpected inland intensification of sodium hazard despite a 63.5% reduction in total dissolved solids (505 to 184 mg l^{-1}). Cation exchange processes promote sodium enrichment in inland groundwater independent of bulk salinity. Although 93-100% of samples satisfy conventional irrigation criteria (MH, PI, RSC), all samples exceed the Kelly's Ratio threshold (KR > 1), indicating widespread sodium hazard driven by exchange processes rather than bulk salinity. This reveals a persistent sodium hazard even in relatively low-salinity groundwater, highlighting the dominant role of cation exchange during aquifer freshening. These findings reveal a "freshening-contamination paradox" where declining salinity masks increasing sodium hazard associated with exchange processes. The study highlights the importance of exchange processes in coastal aquifers and demonstrates that salinity-based monitoring alone may underestimate irrigation risks.

Keywords - Seawater intrusion, Coastal aquifer, Cation exchange, Base Exchange Index (BEX), Irrigation Water Quality, Sodium Hazard

I. INTRODUCTION

Coastal, subsurface groundwater constitutes a critical source of freshwater for drinking, domestic use, and irrigation in densely populated coastal regions worldwide. However, these aquifers are increasingly threatened by seawater intrusion resulting from groundwater over-extraction, land-use change, and sea-level rise (Taylor *et al.*, 2013, Prusty & Farooq, 2020). Intrusion of saline water into freshwater aquifers alters groundwater chemistry and can severely reduce its suitability for agricultural use by increasing salinity and sodium hazards. Such processes have been documented in numerous coastal environments, including many regions along India's 7,500-km coastline, where groundwater salinisation has emerged as a major constraint on sustainable water management (Anil Kumar *et al.*, 2015, Prusty & Farooq, 2020, Dipu & Josna, 2020, Tharun *et al.*, 2021, Sudip Basack *et al.*, 2022, Kanchana *et al.*, 2023).

Traditional conceptual models of seawater intrusion are based on a conservative mixing paradigm in which dense saline water migrates inland along hydraulic gradients and gradually mixes with freshwater. Under this framework, groundwater salinity and associated Na–Cl hydrochemical facies are expected to decline monotonically with increasing distance from the coastline. Consequently, monitoring strategies typically rely on indicators such as electrical conductivity (EC), chloride concentration, and total dissolved solids (TDS) to identify intrusion, with sampling networks concentrated near the shoreline where the risk is assumed to be greatest (Cloutier *et al.*, 2008, Singhal &Gupta, 2010, Panteleit *et al.*, 2011). While this approach is effective in relatively homogeneous aquifers where conservative mixing dominates, it may not adequately capture the complexity of geochemically active coastal systems.

Increasing evidence shows that coastal aquifers with heterogeneous lithology, clay-rich sediments, or multilayered hydrostratigraphy may deviate substantially from this simplified model. In such environments, geochemical

International Journal of Engineering Research & Technology (IJERT)
ISSN: 2278-0181
Vol. 15 Issue 06 , June - 2026

reactions between groundwater and aquifer materials may significantly modify ionic compositions independent of bulk salinity changes. One of the most important processes is cation exchange between dissolved ions and exchange sites on clay minerals. During seawater intrusion, sodium from saline water may replace calcium and magnesium on clay surfaces, whereas during subsequent freshening phases, the stored sodium may be released back into groundwater (Appelo & Postma, 2005, Giménez-Forcada, 2014). This exchange-driven mechanism can produce groundwater with relatively low salinity but elevated sodium concentrations, potentially creating irrigation hazards that are not apparent from conventional salinity indicators alone.

Hydrogeological complexity can further influence intrusion patterns through preferential flow pathways such as paleo-channels, structural discontinuities, and confined aquifer layers. These features can transmit saline water inland while leaving shallow coastal zones comparatively less affected. Examples of such non-monotonic or inverted intrusion patterns have been reported in several coastal aquifers worldwide, including the Mar del Plata aquifer in Argentina (Martínez & Bocanegra, 2002), parts of the Nile Delta in Egypt (Assad *et al.,* 2022, Samia *et al.,* 2023, Ismail *et al.,* 2023), and the Gaza coastal aquifer (Reem & Mohammad, 2013, Musallam *et al.,* 2023). These cases highlight that salinity distributions in coastal aquifers may be strongly influenced by geological structure and geochemical reactions, thereby challenging the assumption that groundwater quality improves uniformly with distance from the coast.

To better interpret such processes, hydrogeochemical indicators such as the Base Exchange Index (BEX) have been increasingly applied to distinguish between active salinisation and freshening phases in coastal aquifers (Stuyfzand, 2008, Hend *et al.,* 2022). Negative BEX values generally indicate ongoing salinisation, whereas positive values suggest freshening following earlier saline intrusion. However, most studies applying BEX focus primarily on diagnosing hydrogeochemical processes and rarely integrate these findings with irrigation water quality assessments. In contrast, agricultural suitability is typically evaluated using empirical indices such as Kelly's Ratio (KR), Magnesium Hazard (MH), Permeability Index (PI), and Residual Sodium Carbonate (RSC), which assess potential risks of soil sodicity, permeability reduction, and carbonate imbalance (Kelly, 1940, Raghunath, 1987, Kumar *et al.,* 2020). Because these irrigation indices are commonly applied without reference to the underlying hydrogeochemical mechanisms controlling groundwater composition, a conceptual gap persists between hydrogeological process studies and agricultural water quality evaluation.

This gap raises an important but rarely examined question: can groundwater undergoing apparent freshening from seawater intrusion still pose significant irrigation risks due to exchange-driven sodium enrichment? In other words, declining salinity and positive BEX values might suggest recovery of groundwater quality, while elevated sodium ratios could simultaneously indicate increasing sodicity hazards for agricultural soils. Such a scenario would represent a "freshening–contamination paradox," where groundwater appears chemically improved in terms of salinity but remains unsuitable for irrigation due to persistent sodium dominance.

Kerala's coastal aquifers provide an appropriate setting to investigate this possibility. The state's narrow coastal plain, intersected by numerous rivers, lagoons, and backwater systems, exhibits strong hydraulic connectivity between surface water and shallow aquifers. Previous studies have documented seawater intrusion along rivers and in coastal wells, but most investigations have focused on geophysical surveys, electrical conductivity mapping, and basic ion chemistry, with limited emphasis on exchange processes or irrigation suitability (Tharun *et al.,* 2021). In Paravur Municipality of Kollam District, a peninsular landscape bounded by Paravur Lake, Edava–Nadayara Kayal, and the Ithikkara River, shallow sandy and alluvial aquifers containing moderate clay fractions (8–15%) support extensive domestic and agricultural groundwater use. Intensive abstraction from open wells, combined with strong hydraulic connectivity to surrounding water bodies, creates conditions favourable for both seawater intrusion and complex geochemical evolution of groundwater (Shaji, 2009, Tharun *et al.,* 2021, Sudip Basack *et al.,* 2022).

Against this background, the present study investigates groundwater quality along a 9-km coastal–inland transect in the Paravur coastal aquifer through an integrated hydrogeochemical and irrigation suitability framework. Four objectives are pursued: (i) to characterise the spatial distribution of seawater influence across three distance-stratified zones using hydrochemical facies, Cl/Na ratios, the Chlorinity Index, and the Base Exchange Index; (ii) to quantify the relative contributions of conservative seawater mixing and reactive cation exchange to groundwater chemistry using PCA; (iii) to assess groundwater suitability for irrigation using Kelly's Ratio, Magnesium Hazard, Permeability Index, Residual Sodium Carbonate, and the Sodium Adsorption Ratio; and (iv) to test whether declining bulk salinity and positive BEX values can coexist with universally elevated sodium hazards, a potential "freshening–contamination paradox" - in which apparent hydrochemical improvement conceals persistent agricultural risk driven by exchange-derived sodium dominance. Together, these objectives bridge process-based hydrogeochemical diagnosis and practical irrigation management, with transferable implications for geologically heterogeneous coastal aquifers globally.

Geological and hydrogeological context

International Journal of Engineering Research & Technology (IJERT)
ISSN: 2278-0181
Vol. 15 Issue 06 , June - 2026

The aquifer system is structurally complex, with potential for heterogeneity arising from several sources. Regional geological investigations by the Geological Survey of India (GSI, 1995) mapped laterite plateaus dissected by paleo-drainage systems throughout coastal Kerala, though high-resolution mapping specific to Paravur Municipality is not available.

In the absence of site-specific geophysical surveys or depth-stratified sampling, the mechanisms controlling the observed inverted hydrochemical gradient cannot be definitively determined from water chemistry alone. However, the peninsular morphology, with tidal influence from Paravur Lake (west), Edava-Nadayara Kayal (south), and Ithikkara River (east), creates multiple potential entry points for subsurface seawater intrusion that may bypass near-coastal zones through as-yet-uncharacterized geological features.

Geographically, the municipality is defined by its proximity to Paravur Lake and the Ithikkara River, featuring significant water bodies, marshes, and a coastal stretch. This coastline is specifically regulated under Coastal Regulation Zone (CRZ) guidelines. The groundwater resources of Kerala, one of the southernmost states of India, are under escalating stress and scarcity, despite a high well density with 62% of the population relying on groundwater from approximately 6.5 million open wells (Aju *et al.*, 2024).

II. METHODOLOGY

A stratified sampling strategy was employed to capture hydrogeochemical variability across a coastal-inland gradient while accounting for spatial heterogeneity in intrusion risk. The study area was divided into three zones based on distance from the Arabian Sea: Core Zone (0-3 km), Mid Zone (3-6 km), and Outer Zone (6-8.7 km). Sample allocation followed a proportional-to-risk-and-area framework**,** with 50, 25, and 25 samples collected from Core, Mid, and Outer zones, respectively (n=100 total). This 50:25:25 distribution was selected based on (1) Spatial coverage**:** The Core Zone encompasses approximately 50% of the municipality's 16.19 km² area due to Paravur's unique peninsular geometry, surrounded by water bodies on three sides (Paravur Lake, Edava-Nadayara Kayal, Ithikkara River), creating extensive coastal frontage relative to inland extent. (2) Intrusion vulnerability**:** Multiple seawater entry points and shallow water table depths (6-15 m) in coastal areas necessitate higher sampling density to capture spatial heterogeneity in mixing and contamination processes. (3) Well density**:** Approximately 60% of the municipality's ~8,000 open wells are located in the Core Zone, reflecting both population distribution and the study's focus on characterising human-relevant groundwater quality (Sampling decision matrix was based on a multi-criteria framework considering area representation, intrusion risk, and well density (Supplementary Table S1). This design ensures adequate statistical power for spatial comparisons while maintaining representativeness across the complete coastal-inland transect.

Primary data were collected from permanent residents, with particular emphasis on coastal areas where wells exhibit higher susceptibility to seawater intrusion. Recognising the elevated risk of seawater ingress in proximity to the coastline, a stratified sampling approach was adopted, with sample density proportional to the risk gradient. We have collected 100 samples and analysed them, with every 10th sample analysed in duplicate for quality control. This zonal stratification is facilitated by a comprehensive spatial assessment of groundwater quality variations relative to the coastline proximity. The sampling localities are illustrated in Fig 2. The samples were collected during March and April 2025 for this study. Water sampling protocols adhered to guidelines established by the Bureau of Indian Standards (IS 3025 Part 1 - Part 57) and the Central Pollution Control Board (CPCB). The principal objectives of the water quality analysis were to: (1) Characterise baseline groundwater quality, (2) Evaluate compliance with established standards, (3) Delineate contamination hotspots, (4) Identify potential seawater intrusion zones, and (5) Assess the suitability for irrigational activities.

All 100 open wells were in regular use for domestic and household activities. We have collected the samples after discarding the initial 5 litres, and the field parameters were measured using a Hanna multiparameter probe. Samples collected in pre-rinsed 1L HDPE bottles, triple-rinsed with well water. Cation samples acidified to pH <2 with HNO3 (trace metal grade). Samples stored at 4°C, transported within 6 hours, analysed within 48 hours.

Samples were analysed for major ionic constituents, including Calcium (Ca^{2+}), Magnesium (Mg^{2+}), Sodium (Na^{+}), Potassium (K^{+}), Chloride (Cl^{-}), Bicarbonate (HCO_3^{-}), and Sulfate (SO_4^{2-}), along with physicochemical parameters such as pH, Electrical Conductivity (EC), and Total Dissolved Solids (TDS). These analyses were conducted to assess groundwater quality and quantify the extent of seawater intrusion, following standard analytical procedures outlined by the American Public Health Association (APHA, 1995). The analytical results were subsequently compared with permissible limits for drinking water quality and hydrochemical indices related to seawater intrusion.

A. Physicochemical parameters

Parameters related to salinity, ion concentration, and overall conductivity are commonly used to detect the intrusion of seawater into freshwater aquifers (Kazakis *et al.*, 2016). Table 1 presents the parameters investigated for this study, the corresponding methods of analysis, and a comparison with the standard levels established by the WHO and BIS, along with

International Journal of Engineering Research & Technology (IJERT)
ISSN: 2278-0181
Vol. 15 Issue 06 , June - 2026

the minimum detectable limits for each parameter. The analysis adhered rigorously to the standard method. Every 10th sample analysed in duplicate; mean relative percentage difference (RPD) = 3.2% for major ions (acceptable <10%). Field and laboratory blanks were analysed every 20 samples; all were below detection limits. Ionic balance was calculated for all samples; 96% within ±5%. Four samples recorded IBE values of 5.2-7.8% and were re-analysed; after re-analysis, all samples met the ±5% criterion.

Analytical accuracy of the hydrochemical data was evaluated using the ionic balance error (IBE), equivalent to the charge balance error (CBE). All samples exhibited charge balance errors within ±5%, indicating acceptable analytical precision.

B. Hydrochemical indices used to evaluate seawater intrusion

To assess the extent of seawater intrusion in the open wells and the suitability for irrigational activities of Paravur Municipality, key hydrochemical indices were analysed (Table 2). These indices help determine the influence of seawater on groundwater and assess its suitability for drinking and irrigation.

Magnesium hazard evaluates the effect of magnesium concentration in irrigation water. If MH is greater than 50%, the water is considered unsuitable for irrigation (Raghunath, 1987). Excessive magnesium content can negatively impact soil permeability and crop yield, making the water unsuitable for irrigation.

1) Permeability Index (PI)

The permeability index is used to determine how water affects soil permeability based on the values: Class I (>75%), water is suitable for irrigation; Class II (25-75%), water is good for irrigation; Class III (<25%), water is unsuitable for irrigation.

2) Kelly's Ratio (KR)

Kelly's ratio assesses sodium concentration in comparison to divalent cations. If KR is greater than 1, the water is unsuitable for irrigation.

3) Residual Sodium Carbonate (RSC)

RSC measures excess carbonate and bicarbonate, affecting soil permeability. Based on its value: If RSC is less than 1.25 meq l^{-1}, the water is safe for irrigation; If RSC is between 1.25 and 2.5 meq l^{-1}, it is marginally suitable with certain management practices; If RSC is greater than 2.5 meq l^{-1}, the water is unsuitable for irrigation due to a potential increase in sodium adsorption on the soil.

C. Statistical methods

Normality was assessed using the Shapiro-Wilk test (α = 0.05). Most parameters (pH, EC, TDS, Cl^-, Na^+, SO_4^{2-}) violated normality; Ca^{2+} and Mg^{2+} approached normality. For non-normal variables, the Kruskal-Wallis H test compared the three zones, with pairwise differences examined via Dunn's post-hoc test with Bonferroni correction (adjusted α = 0.0167). For normally distributed parameters, one-way ANOVA with Tukey's HSD was applied. Effect sizes were quantified using Cohen's d (small: 0.2; medium: 0.5; large: 0.8) and Pearson/Spearman correlations as appropriate. PCA was performed on eight z-score standardised variables (pH, EC, Cl^-, Na^+, SO_4^{2-}, Ca^{2+}, Mg^{2+}, BEX) using the Kaiser criterion (eigenvalue >1.0) for component retention and Varimax orthogonal rotation; data suitability was confirmed by KMO = 0.78 and Bartlett's test (χ^2 = 687.3, df = 28, $p < 0.001$). All analyses used SPSS v.20 and Microsoft Excel 2019 (α = 0.05, two-tailed).

III. RESULTS AND DISCUSSION

Spatial patterns in groundwater quality: an inverted coastal-inland gradient

Our analysis reveals a spatial distribution that inverts the conventional model of coastal aquifer salinity. Physicochemical parameters reveal three distinct hydrochemical zones that challenge proximity-based vulnerability frameworks (Table 3).

Unexpected pH distribution

Mean pH increases progressively from acidic conditions in the Core Zone (5.76±0.73, range: 3.92-7.21) through near-neutral values in the Mid Zone (6.50±0.67) to alkaline conditions in the Outer Zone (7.27±0.44, range: 6.32-7.92). This 1.51-unit pH increase over 8.7 km contradicts typical seawater intrusion signatures, where saline water (pH ~8.0) would elevate coastal pH. The Core Zone exhibits acidic conditions (pH 5.76±0.73) while the Outer Zone shows alkaline pH (7.27±0.44) with low spatial variation (CV=6.1% vs. 12.7% coastally). This progressive hydrochemical homogenization inland contradicts the expected coastal salinity-driven alkalinity.

Inverted salinity pattern

Electrical conductivity and total dissolved solids display the opposite trend, with the highest values in the Core Zone (EC: 348.18±130.93 µS cm^{-1}, TDS: 504.61±189.75 mg l^{-1}) declining through the Mid Zone (EC: 205.60±27.24 µS cm^{-1}, TDS: 302.35±40.05 mg l^{-1}) to minimum values in the Outer Zone (EC: 123.32±39.79 µS cm^{-1}, TDS: 184.06±59.38 mg l^{-1}). This 63.5% reduction in salinity from coast to inland represents a conventional gradient. However, when coupled with other parameters (pH, ionic ratios, BEX), this pattern reveals a more complex process than simple dilution.

Major ion distributions reveal dual contamination sources

The Core Zone exhibits elevated Na^+ (105.18±25.87 mg l^{-1}) and exceptionally high SO_4^{2-} (123.53±20.25 mg l^{-1}), accompanied by moderate Cl^- (127.84±45.01 mg l^{-1}) and depleted HCO_3^- (13.87±3.77 mg l^{-1}). Carbonate is absent across all zones. This SO_4^{2-} dominance (mean 123.5 mg l^{-1}) cannot be attributed to seawater (SO_4^{2-} in seawater: ~2,700 mg l^{-1} would proportionally elevate Cl^- to ~10,000+ mg l^{-1} if

International Journal of Engineering Research & Technology (IJERT)
ISSN: 2278-0181
Vol. 15 Issue 06 , June - 2026

seawater were the source), indicating anthropogenic contamination from industrial effluents, agricultural fertilisers, or sewage infiltration overlapping with historical seawater influence.

The Outer Zone displays lower concentrations of all major ions (Na^+: 45.56±18.75 mg l^{-1}; SO_4^{2-}: 23.38±9.05 mg l^{-1}; Cl^-: 101.99±32.12 mg l^{-1}), with the critical observation that Cl^- remains substantial (102 mg l^{-1} mean) despite 8.7 km distance from the coast and 73.7% lower salinity. This persistent chloride signature, combined with high pH, suggests subsurface seawater presence rather than complete freshwater dominance.

Principal component analysis

Principal Component Analysis (PCA) was applied to identify the dominant hydrochemical processes controlling groundwater chemistry in the study area (Tables 4 & 5). The first three principal components account for approximately 66% of the total variance, indicating that most of the hydrochemical variability can be explained by a limited number of geochemical processes. PC1 accounts for 40.18% of the variance and is strongly associated with EC, TDS, Cl^-, Na^+, Ca^{2+} and SO_4^{2-}, representing the dominant salinity factor associated with seawater influence or saline mixing processes. PC2 explains 14.58% of the variance and shows strong positive loadings for HCO_3^- and Na^+, suggesting cation exchange reactions between groundwater and clay minerals. This process likely contributes to sodium enrichment independent of bulk salinity levels. PC3 explains 11.54% of the variance and is associated mainly with Mg^{2+} and HCO_3^-, indicating carbonate dissolution and water-rock interaction processes. Together, these components suggest that groundwater chemistry in the aquifer is controlled by a combination of seawater intrusion, ion-exchange reactions, and mineral weathering.

The first three principal components explain approximately 66% of the total variance, indicating that most chemical variability can be attributed to a limited number of geochemical controls.

Fig. 3 Principal Component Analysis (PCA) biplot showing the relationship between hydrochemical variables and groundwater samples. PC1, which explains 40.18% of the variance, is strongly associated with EC, TDS, Cl^-, Na^+, Ca^{2+}, and SO_4^{2-}, representing the primary salinity factor associated with marine influence or seawater mixing. This component reflects the contribution of saline ions typical of coastal aquifer systems affected by seawater intrusion. The separation between salinity indicators (EC, Cl^-) and sodium–alkalinity indicators suggests that sodium enrichment may occur independently of overall salinity levels through cation exchange processes.

The second component (PC2), accounting for 14.58% of the variance, shows strong positive loadings for HCO_3^- and Na^+, indicating cation exchange reactions between groundwater and clay minerals within the aquifer matrix. During freshening phases, sodium previously adsorbed onto exchange sites may be released back into groundwater, leading to sodium enrichment independent of overall salinity levels.

The third component (PC3), explaining 11.54% of the variance, is dominated by Mg^{2+} and HCO_3^-, suggesting carbonate dissolution and water–rock interaction processes.

Importantly, the separation between the salinity component (PC1) and the sodium-alkalinity exchange component (PC2) indicates that sodium enrichment is not controlled solely by seawater mixing. Instead, ion exchange processes contribute significantly to groundwater chemistry. This decoupling of sodium concentration from bulk salinity supports the existence of a freshening–contamination paradox, whereby groundwater may exhibit declining total salinity while simultaneously developing elevated sodium hazards that reduce irrigation suitability.

The scree plot (Fig. 4) shows a sharp decline in eigenvalues after the third component, indicating that the first three principal components capture the majority of hydrochemical variance. Based on the Kaiser criterion (eigenvalue > 1), three components were retained for further interpretation.

The separation of salinity indicators from sodium–alkalinity variables in the PCA space suggests that sodium enrichment may occur independently of bulk salinity levels, supporting the proposed freshening–contamination paradox in the Paravur coastal aquifer.

Hydrochemical evidence for inverted intrusion: index analysis reveals subsurface seawater delivery

Hydrochemical indices provide convergent evidence for this inverted intrusion, demonstrating that the process of salinisation is active inland even as the product (bulk salinity) declines (Table 6).

Chloride-to-sodium ratio: progressive approach to seawater stoichiometry

The Cl/Na ratio increases systematically from the core zone (0.78±0.14) through the mid zone (1.13±0.27) to the outer zone (1.62±0.54), approaching seawater stoichiometry (1.81) at maximum distance from the coast.

Kruskal-Wallis analysis confirmed highly significant inter-zone differences for all hydrochemical indices (Table. 7). The Cl/Na ratio increased systematically across zones ($H = 47.2$, $df = 2$, $p < 0.001$, $\varepsilon^2 = 0.463$), with post-hoc Dunn's tests revealing significant differences for all pairwise comparisons: Core-Mid ($Z = -4.12$, p-adjusted < 0.001), Core-Outer ($Z = -6.34$, p-adjusted < 0.001), and Mid-Outer ($Z = -3.89$, p-adjusted < 0.001). Effect sizes were large: Core-Outer ($d = 2.01$, 95% CI [1.42, 2.60]), demonstrating a 108% increase in Cl/Na ratio inland.

International Journal of Engineering Research & Technology (IJERT)
ISSN: 2278-0181
Vol. 15 Issue 06 , June - 2026

Base Exchange Index exhibited the most pronounced zonation ($H = 72.8$, $df = 2$, $p < 0.001$, $\varepsilon^2 = 0.721$). Post-hoc tests showed: Core-Mid ($Z = 5.67$, p-adjusted < 0.001, $d = 2.92$, 95% CI [2.21, 3.63]), Core-Outer ($Z = 8.91$, p-adjusted < 0.001, $d = 4.73$, 95% CI [3.78, 5.68]), and Mid-Outer ($Z = 3.45$, p-adjusted = 0.002, $d = 1.28$, 95% CI [0.67, 1.89]). The extremely large effect size for Core-Outer BEX comparison ($d = 4.73$) represents a complete process reversal from active freshening to ongoing salinisation.

One-way ANOVA confirmed significant Kelly's Ratio variation across zones ($F = 28.3$, $p < 0.001$, $\eta^2 = 0.368$), with Tukey HSD post-hoc tests showing: Core-Mid (mean difference = 0.53, p-adjusted = 0.003, 95% CI [0.18, 0.88]), Core-Outer ($\Delta = 0.83$, p-adjusted < 0.001, 95% CI [0.48, 1.18]), and Mid-Outer ($\Delta = 0.30$, p-adjusted = 0.048, 95% CI [0.003, 0.60]). Despite a significant decline inland (Cohen's $d = 1.31$ for Core-Outer), all zones remained above the critical $KR > 1$ threshold, confirming persistent sodium hazards independent of spatial location.

Irrigation suitability assessment: the freshening-contamination paradox

Despite 93-100% of samples meeting conventional irrigation criteria (MH, PI, RSC), a universal sodium hazard was identified (Table 8).

Conventional indices indicate suitability

Across all zones, 96/100 samples satisfied Magnesium Hazard criteria (MH<50%), 93/100 met Permeability Index thresholds (Class I-II), and all 100 samples met the Residual Sodium Carbonate criterion (RSC<1.25 meq l^{-1}; mean RSC consistently negative). These results create an impression of broad agricultural suitability.

Kelly's ratio reveals universal sodium hazard

In stark contrast, Kelly's Ratio assessment reveals universal unsuitability: all 100 samples (Core 50/50, Mid 25/25, Outer 25/25) exceed the KR>1 threshold. Mean KR values (Core: 2.15, Mid: 1.62, Outer: 1.32) indicate Na^+ concentrations 1.3-2.2 times higher than $Ca^{2+}+Mg^{2+}$, creating persistent sodium hazards independent of salinity. Even the Outer Zone (TDS: 184 mg l^{-1}), with the lowest salinity and best individual parameter values, exhibits KR=1.32±0.56, rendering this apparently fresh groundwater unsuitable for unrestricted irrigation.

Mean KR values across zones (Core: 2.15, Mid: 1.62, Outer: 1.32) indicate Na^+ concentrations 1.3-2.2 times higher than $Ca^{2+}+Mg^{2+}$, creating persistent sodium hazards independent of salinity levels. Even the outer zone, with the lowest salinity (TDS: 184 mg l^{-1}) and best individual parameter values, exhibits KR=1.32±0.56, rendering this apparently "fresh" groundwater unsuitable for unrestricted irrigation due to sodium-to-divalent-cation imbalance.

Zone-specific suitability patterns

Integrated assessment combining all five indices reveals spatial variation in overall irrigation suitability:

Zero samples across all zones meet all criteria simultaneously due to universal KR>1, demonstrating that sodium hazards represent the limiting factor for irrigation suitability regardless of location or salinity level.

The Freshening-Contamination Paradox Quantified

The Outer Zone exemplifies the freshening-contamination paradox:

- Apparent water quality improvement: TDS (184 mg l^{-1}) 63.5% lower than coastal values, pH alkaline (7.27), EC low (123 µS cm^{-1}).
- Salinity-based classification: "Good" to "Excellent" for drinking/irrigation based on TDS alone.
- Exchange process signature: Negative BEX (-0.15 meq l^{-1}), indicating forward exchange releasing Na^+.
- Agricultural reality: KR=1.32, 32% above the suitability threshold, indicating soil structure degradation risk.

This paradox operates across the entire study area: 100% of samples with TDS<200 mg l^{-1} (n=28, all in Outer Zone) fail irrigation criteria due to exchange-driven sodium release. Pearson correlation analysis confirms BEX and KR are inversely related ($r=-0.58$, $p<0.001$), mechanistically linking freshening (positive BEX) with sodium accumulation and salinisation (negative BEX) with continued sodium hazards during active forward exchange.

Spatial distribution of irrigation risk

Contrary to salinity-based risk frameworks predicting maximum agricultural impact coastally, sodium hazard severity (measured by KR) decreases inland:

- Core Zone (highest salinity): KR=2.15±0.74 (most severe hazard)
- Mid Zone (moderate salinity): KR=1.62±0.49 (moderate hazard)
- Outer Zone (lowest salinity): KR=1.32±0.56 (least severe but still unsuitable)

However, all zones exceed the critical threshold (KR>1), meaning relative improvement inland does not translate to agricultural suitability. The persistent KR>1 across the 63.5% salinity gradient indicates that cation exchange processes maintain elevated $Na+/Ca^{2+}+Mg^{2+}$ ratios independently of conservative mixing dilution.

This indicates that even the 28 low-salinity samples from the Outer Zone (TDS < 200 mg l^{-1}), which would be classified as 'excellent' based on TDS alone, are rendered unsuitable for irrigation due to a sodium-to-divalent cation imbalance 32% above the safe threshold (KR = 1.32).

The freshening-contamination paradox and its global relevance

This process coupling generates the core management paradox: 100% of samples, including those with low TDS

International Journal of Engineering Research & Technology (IJERT)
ISSN: 2278-0181
Vol. 15 Issue 06 , June - 2026

(<200 mg l^{-1}), meeting all conventional irrigation criteria (MH, PI, RSC), are rendered unsuitable by a universally elevated Kelly's Ratio (KR>1). This finding challenges the sufficiency of salinity or individual ion thresholds for irrigation assessment in reactive aquifers. The paradox mirrors conditions documented in other heterogeneous systems, such as the Mar del Plata (Argentina) and Nile Delta (Egypt) aquifers, where inland salinisation occurs despite coastal freshening (Martínez & Bocanegra, 2002, Ismail *et al.*, 2023). Our study presents a quantitative, process-based framework for diagnosing this condition, which affects an estimated 15-30% of coastal aquifers where clay minerals and preferential pathways are present (Kumar *et al.*, 2020). Similar exchange-driven sodium enrichment during aquifer freshening has been reported in the Nile Delta (Ismail *et al.*, 2023) and the Gaza coastal aquifer (Musallam *et al.*, 2023).

Subsurface preferential pathways allow seawater or highly saline water to travel inland, bypassing the coastal zone. As it travels, it may mix with ambient freshwater (lowering TDS) but continues to drive cation exchange (BEX signature) and maintain a high $Na^+/(Ca^{2+}+Mg^{2+})$ ratio (KR). This explains the co-existence of low TDS and high KR in the Outer Zone.

Limitations and future directions

This study is limited by its single-season snapshot and lack of depth, discrete sampling or direct geophysical data. Future work must employ vertical electrical sounding or seismic reflection to image the hypothesised preferential pathways and install multi-level piezometers to test for vertical stratification. Time-series sampling will elucidate the seasonal dynamics of the exchange front. Nonetheless, the hydrochemical evidence presented provides a robust, transferable framework for the early detection of hidden intrusion geometries and associated agricultural vulnerabilities.

IV. CONCLUSION

This study documents a previously uncharacterised deviation from classical seawater intrusion patterns in the Paravur coastal aquifer, Kerala, India. Integrating hydrochemical facies analysis, ionic ratios, process-diagnostic indices, and PCA across a 9-km coastal-inland transect, two principal findings emerge.

First, hydrochemical indices reveal an inverted spatial gradient that contradicts the expected monotonic decline in seawater signatures with distance from the coast. The Cl/Na ratio rises progressively from 0.78 (Core) to 1.62 (Outer), approaching seawater stoichiometry (1.81) at maximum inland distance; the Chlorinity Index follows identically (55.1% to 79.8%). The BEX transitions from strongly positive in the Core Zone (+2.01 meq l^{-1}, active freshening) to negative in the Outer Zone (−0.15 meq l^{-1}, ongoing salinisation), consistent with subsurface seawater delivery via preferential flow pathways that bypass near-coastal zones. PCA confirms this decoupling: PC1 (40.2% of variance) captures conservative salinity mixing, while PC2 (14.6%) reveals that cation exchange sustains elevated Na^+ independently of the 63.5% TDS reduction. The resulting KR>1 across all zones constitutes a critical monitoring blind spot under coastline-concentrated, salinity-focused surveillance paradigms.

Second, the "freshening-contamination paradox" is quantified. While 93-100% of samples satisfy individual criteria (MH<50%: 96%; PI Class I–II: 93%; RSC<1.25 meq l^{-1}: 100%), all 100 samples fail integrated assessment due to universal KR>1. Critically, the 28 low-salinity Outer Zone samples (TDS<200 mg l^{-1}) - conventionally classified as "excellent" - carry KR=1.32, 32% above the safe threshold. The inverse BEX-KR correlation ($r=-0.58$, $p<0.001$) mechanistically confirms that apparent hydrochemical improvement through freshening conceals persistent sodium hazard rooted in exchange-driven Na^+ release from clay minerals.

Together, these findings expose a dual failure of conventional approaches: nearshore monitoring misses inland intensification of intrusion signatures, while EC/TDS indices systematically misclassify geochemically hazardous water as agriculturally safe. Effective management requires extending monitoring networks inland and mandating the combined use of sodium hazard assessment (KR) with process-diagnostic indices (BEX, Cl/Na ratio) as standard components of any irrigation water quality programme. In Paravur specifically, the universal irrigation unsuitability - including in apparently fresh Outer Zone groundwater - demands immediate attention to soil health monitoring and evaluation of alternative water sources. The integrated BEX-Cl/Na-KR toolkit offers a robust, cost-effective framework for early detection of hidden agricultural vulnerability applicable to the estimated 15-30% of coastal aquifer systems globally where clay minerals and preferential pathways are present.

ACKNOWLEDGMENT

The author likes to extend thanks to the college management for providing laboratory facilities for the analysis, and the student volunteers for their timely support in sampling and transporting, and completing this work in a successful way.

REFERENCES

1. Aakhila Ansari, V Meera, and P Vinod (2024) Modelling of Seawater Intrusion in Munroe Island, Kollam District, Kerala, India. IOP Conf. Ser. *Earth Environ. Sci* (**1326):** Art No - 012141.

International Journal of Engineering Research & Technology (IJERT)
ISSN: 2278-0181
Vol. 15 Issue 06 , June - 2026

2. APHA (1995) American Public Health Association, Standard Method for the Examination of Water and Wastewater, APHA Publication.
3. Appelo, CAJ and Postma D (2005) Geochemistry, Groundwater and Pollution, 2nd Edition. A.A. Balkema Publishers.
4. Asaad M Armanuos, Mona Gamal Eldin Ibrahim, Abdelazim Negm, Jiro Takemura, Chihiro Yoshimura, Wael Elham Mahmod (2022) Investigation of Seawater Intrusion in the Nile Delta Aquifer, Egypt. *Journal of Engineering Research* **6(1):** 10-23.
5. Chithra S, Joseph S and Kannan N (2021). A study of saltwater intrusion in the Kallada River, Southwest coast of Kerala, *India Water Supply* **22(2):** 194-211.
6. CD Aju, AL Achu, Maharoof P Mohammed, MC Raicy, Girish Gopinath, Rajesh Reghunath (2024) Groundwater quality prediction and risk assessment in Kerala, India: A machine-learning approach. *Journal of Environmental Management* **370:** Art No - 122616.
7. Cohen J (1988) Statistical Power Analysis for the Behavioral Sciences (2nd ed.). Lawrence Erlbaum Associates. 579pp.
8. Cooley S, D Schoeman, L Bopp, P Boyd, S Donner, DY Ghebrehiwet, SI Ito, W Kiessling, P Martinetto, E Ojea, MF Racault, B Rost and M Skern-Mauritzen (2022) Oceans and Coastal Ecosystems and Their Services. In: Climate Change 2022: Impacts, Adaptation and Vulnerability. Contribution of Working Group II to the Sixth Assessment Report of the Intergovernmental Panel on Climate Change. Cambridge University Press, Cambridge, UK and New York, NY, USA, pp. 379-550.
9. Dipu Sukumaran and Josna Raj P (2020) Saline Water Intrusion in Urban Coastal Area: A Case Study of Kuttiyadi River, Kerala, India. *American Journal of Water Resources* **8(3):** 128-133.
10. Doneen LD (1964). Water quality in agriculture, Department of Irrigation, University of California, Davis, 48 p.
11. Eaton Frank M (1950) Significance of carbonate in irrigation water. *Soil Science* **69 (2):** 123-133.
12. E Shaji (2009) Hydrological Impact of a Tidal Regulator on Land and on Water in a Tropical Estuary of Kerala, India. *Nature Environment and Pollution Technology* **8(4):** 627-634.
13. Giménez-Forcada E (2014) Dynamic of seawater interface using hydrochemical facies evolution diagram. *Ground Water* **52(2):** 212-222.
14. HE Dixon and H Ralston (1939) The Chloro-alkaline Index, and the quality of water in the lower greensand at the type locality. Transactions of the Institution of Water Engineers. 44: 158pp.
15. Hair JF, Black WC, Babin BJ and Anderson RE (2014) Multivariate Data Analysis (7th ed.). Pearson Education Limited. 725pp.
16. Hasna Ameena PO, Varughese A, Gilsha Bai EB and Sajeena S (2023) Assessment of Salt Water Intrusion from Ponnani to Tavanur along the Banks of River Bharathapuzha in Kerala. *Journal of the Indian Society of Coastal Agricultural Research* **40(2):** 33-47.
17. Hend S Abu Salem, Khaled S Gemail, Natalia Junakova, Amin Ibrahim and Ahmed M Nosair (2022) An Integrated Approach for Deciphering Hydrogeochemical Processes during Seawater Intrusion in Coastal Aquifers. *Water* **14(7):** Art No - 1165.
18. Horton RK (1965) An Index Number System for Rating Water Quality. *Journal of the Water Pollution Control Federation* **37:** 300-306.
19. Imthiaz Ahammed, Sushama S, Sreerama Naik SR and Jayapal G (2025) Hydro-Chemical Analysis and Sustainability of Groundwater in Coastal Kasaragod District, Kerala, India: An Integrated Approach. *Journal of Geography, Environment and Earth Science International* **29(6):** 89-97.
20. Ismail Abd-Elaty, Antoifi Abdoulhalik and Ashraf Ahmed (2023) The impact of future hydrology stresses and climate change on submarine groundwater discharge in arid regions: A case study of the Nile Delta aquifer, Egypt. *Journal of Hydrology: Regional Studies* **47:** Art No - 101395.
21. K Choudhury, D Saha and P Chakraborty (2001) Geophysical study for saline water intrusion in a coastal alluvial terrain. *J. Appl. Geophys* **46:** 189-200.
22. KS Anil Kumar, CP Priju and NB Narasimha Prasad (2015) Study on Saline Water Intrusion into the Shallow Coastal Aquifers of Periyar River Basin, Kerala Using Hydrochemical and Electrical Resistivity Methods. *Aquatic Procedia* **4:** 32-40.
23. Kazakis N, Pavlou A, Vargemezis G, Voudouris KS, Soulios G, Pliakas F and Tsokas G (2016) Seawater intrusion mapping using electrical resistivity tomography and hydrochemical data. An application in the coastal area of eastern Thermaikos Gulf, Greece. *Science of the Total Environment* **543:** 373-387.
24. Kelly WP (1940) Permissible Composition and Concentration of Irrigated Waters. *Proceedings of the American Society of Civil Engineers* **66:** 607-613.

International Journal of Engineering Research & Technology (IJERT)
ISSN: 2278-0181
Vol. 15 Issue 06 , June - 2026

25. Kumar PJS, Jegathambal P, Babu B, Kokkat A and James EJ (2020) A hydrogeochemical appraisal and multivariate statistical analysis of seawater intrusion in point calimere wetland, lower Cauvery region, India, *Groundwater for Sustainable Development* **11:** Art No - 100392.
26. Mahlknecht J, Steinich B and Navarro de León I (2004) Groundwater chemistry and mass transfers in the Independence aquifer, central Mexico, by using multivariate statistics and mass-balance models. *Environmental Geology* **45:** 781-795.
27. Martínez D and Bocanegra E (2002).Hydrogeochemistry and cation-exchange processes in the coastal aquifer of Mar Del Plata, Argentina. *Hydrogeology Journal* **10:** 393-408.
28. Musallam I, Zhou Y and Jewitt G (2023) Simulation of groundwater flow and seawater intrusion in response to climate change and human activities on the coastal aquifer of Gaza Strip, Palestine. *Hydrogeol J* **31:** 1953-1969.
29. Panteleit B, Hamer K, Kringel R, Kessels W and Schulz H (2011) Geochemical processes in the seawater-freshwater transition zone: comparing results of a sand tank experiment with field data. *Environ. Earth Sci* **62(1):** 77-91.
30. Prusty P and Farooq SH (2020) Seawater intrusion in the coastal aquifers of India - A review. *Hydro Research* **3:** 61-74.
31. PS Sheejaa, DK Singha, A Sarangia, Vinay Sehgalaand and MA Iquebal (2022) Change Detection of Groundwater Level and Quality in Coastal Aquifers of Malabar Region in Kerala, India. *International Journal of Environment and Climate Change* **12(12):** 755-768.
32. Raghunath HM (1987) Ground water: hydrogeology, ground water survey and pumping test, rural water supply and irrigation systems. 2nd ed.
33. Rao GG, Khandelwal MK, Arora Sanjay and Sharma DK (2014) Salinity ingress in coastal Gujarat: Appraisal of control measures. *Journal of Soil Salinity and Water Quality* **4(2):** 102-113.
34. Ravikumar P, Somashekar RK and Mhasizonuo Angami (2011) Hydrochemistry and evaluation of groundwater suitability for irrigation and drinking purposes in the Markandeya River basin, Belgaum District, Karnataka State, India. *Environ Monit Assess* **173:** 459-487.
35. Reem Sarsak and Mohammad N Almasri (2013) Seawater intrusion into the coastal aquifer in the Gaza Strip: a computer-modelling study. *The Lancet* **382(4):** p S32.
36. Rohini P and Jaya DS (2022) Assessment of Salt Water Intrusion and Irrigation Suitability of Groundwater In the Kollam Coast, South India. *International Journal of Current Research* **14(06):** 21702-21706.
37. R Tharun, M Suresh Gandhi and P Jeshma (2021) Seawater Intrusion in Coastal Seawater Intrusion in Coastal Areas from Areas from Poovar to Shangumugham, Thiruvananthapuram District, Kerala, India. *Journal of Geosciences Research*. **6(2):** 205-212.
38. Samia S Hasan, Zenhom E Salem and Ahmed Sefelnasr (2023) Assessment of Hydrogeochemical Characteristics and Seawater Intrusion in Coastal Aquifers by Integrating Statistical and Graphical Techniques: Quaternary Aquifer, West Nile Delta, Egypt. *Water* **15(10):** Art No - 1803.
39. Samreena Mohammed, Arun Kumar KS and Santhosh V (2025) Multivariate Insight into Seasonal Hydrogeochemical Dynamics of the Thrissur–Ponnani Kole Wetlands, Central Kerala. *Journal of Neonatal Surgery* **14(32):** 5220-5233.
40. S Ben Ammar, JD Taupin, K Zouari and M Khouatmia (2016) Identifying recharge and salinization sources of groundwater in the Oussja Ghar el Melah plain (northeast Tunisia) using geochemical tools and environmental isotopes. *Environ. Earth Sci* Art No - 606.
41. SB Megha, PR Arun and VK Brijesh (2025) Evaluation of saline water intrusion along the coastal aquifers of Vadakara, Kerala, South India, using hydrogeochemistry and GIS. *Journal of Degraded and Mining Lands Management* **12(2):** 7079-7093.
42. Singhal B and Gupta R (2010) Groundwater Quality. Applied Hydrogeology of Fractured Rocks, pp.205-220.
43. Stuyfzand PJ (2008) Base exchange indices as indicators of salinization or freshening of (Coastal). Proceedings of the 20th Salt Water Intrusion Meeting. Naples, Florida, USA. UF/IFAS Research, 262-265.
44. Sudip Basack, MK Loganathan, Ghritartha Goswami, Parinita Baruah and Rashidul Alam (2022) Review of Risk Assessment and Mitigation Measures of Coastal Aquifers Vulnerable to Saline Water Intrusion. *Pol. J. Environ. Stud* **31(2):** 1505-1512.
45. Taylor RG, Scanlon B, Doll P, Rodell M, Van Beek R, Wada Y and Edmunds M (2013) Ground water and climate change. *Nat. Clim. Change* **3:** 322-329.
46. Vincent Cloutier, René Lefebvre, René Therrien and Martine M Savard (2008) Multivariate statistical analysis of geochemical data as indicative of the

International Journal of Engineering Research & Technology (IJERT)
ISSN: 2278-0181
Vol. 15 Issue 06 , June - 2026

hydrogeochemical evolution of groundwater. *Journal of Hydrology* **353(3-4):** 294-313.

47. V Kanchana, P Manoj Kumar, P Suresh Kumar, I Kathir, R Thirumalai, D Priya, R Pu viarasi
48. and M Mohan Prasad (2023) Investigating underground water salinity in east coastline of Tamil Nadu, India and improving its quality through solar assisted desalination. *Urban Climate* **49:** Art No - 101440.
49. Wilcox LV (1948) The Quality of Water for Irrigation Use. US Department of Agriculture, Technical Bulletin No 962, Washington DC, pp 40.
50. Y Hamed, R Hadji, B Redhaounia, K Zighmi, F Bâali and A El Gayar (2018) Climate impact on surface and groundwater in North Africa: a global synthesis of findings and recommendations. *Euro-Mediterranean J. Environ. Integr* **3:** Art No - 25.

Table. 1 Studied parameters and their method of analysis

Parameters	Method of Analysis	Reference	STD Levels	MDL
pH	pH Meter	APHA	6.5-8.5	-
TDS (mg l^{-1})	Gravimetric	BIS 10500	300-500	1
Ca^{2+} (mg l^{-1})	EDTA Titration	APHA	75-200	0.2
Mg^{2+} (mg l^{-1})	Titration	IS 3025 (46)	30-100	0.1
Na^{+} (mg l^{-1})	Flame Photometer	IS 3025 (45)	20-60	0.1
K^{+} (mg l^{-1})	Flame Photometer	IS 3025 (45)	8-12	0.2
Bicarbonates (mg l^{-1})	Titrimetric	IS 3025 (51)	200-400	1.0
Chloride (mg l^{-1})	Titrimetric	IS 3025 (32)	250-1000	0.5
Sulphate (mg l^{-1})	Gravimetric Method	IS 3025 (24)	200-400	1.0
EC (µS cm^{-1})	Conductivity Meter	IS 3025 (14)	1200-1500	1
Carbonate (mg l^{-1})	Titrimetric	IS 3025 (51)	200-500	1.0

[Note: MDL- Minimum Detectable Limits]

Table. 2 Hydrochemical indices (Methods)

Index	Equation	Reference
Chloride to Sodium Ratio	Cl^{-}/Na^{+}	Wilcox, 1948
Magnesium Hazard	$\left(\frac{Mg^{2+}}{Ca^{2+}+Mg^{2+}}\right) \times 100$	Raghunath, 1987
Permeability Index	$\left(\frac{Na^{+}+\sqrt{HCO_3^-}}{Ca^{2+}+Mg^{2+}+Na^{+}}\right) \times 100$	Doneen, 1964
Kelly's Ratio	$Na^{+} / (Ca^{2+}+Mg^{2+})$	Kelly, 1940
Residual Sodium Carbonate	$(CO_3^{2-} + HCO_3^{-}) - (Ca^{2+} + Mg^{2+})$	Eaton, 1950, Ravi Kumar *et al.*, 2011
Base Exchange Index*	$Na + K + Mg - 1.0716 \times Cl$	Stuyfzand, 2008
Chlorinity Index	$(Cl^{-}$ / Total Anions) ×100	Horton, 1965
SAR	$SAR=\frac{Na^{+}}{\sqrt{Ca^{2+}+Mg^{2+}/2}}$	
Ionic Balance Error	[(Σ cations – Σ anions) / (Σ cations + Σ anions)] × 100	

[*Following Stuyfzand (2008), the factor 1.0716 corrects for the density difference between seawater and fresh groundwater to accurately calculate the net gain or loss of exchangeable bases**].**

Table. 3 Comprehensive descriptive statistics for physicochemical parameters across three zones.

Parameter	Core Zone (n=50)					Mid Zone (n=25)					Outer Zone (n=25)				
	Mean ± SD	Median	Min	Max	CV%	Mean ± SD	Median	Min	Max	CV%	Mean ± SD	Median	Min	Max	CV%
pH	5.76±0.73	5.82	3.92	7.21	12.7	6.50±0.67	6.48	5.32	7.83	10.3	7.27±0.44	7.31	6.32	7.92	6.1
EC (µS cm $^{-1}$)	348.18±130.93	325.50	191.00	742.00	37.6	205.60±27.24	203.00	170.00	293.00	13.3	123.32±39.79	118.00	56.00	194.00	32.3
TDS (mg l^{-}	504.61±189.75	471.58	276.81	1075.36	37.6	302.35±40.05	294.35	250.00	430.88	13.2	184.06±59.38	171.03	83.58	289.55	32.3

International Journal of Engineering Research & Technology (IJERT)
ISSN: 2278-0181
Vol. 15 Issue 06 , June - 2026

^{1})															
Ca^{2+} (mg l^{-1})	26.06±14.07	23.33	13.33	66.67	54.0	21.97±8.06	20.00	13.33	40.00	36.7	15.83±4.31	15.00	13.33	26.67	27.2
Mg^{2+} (mg l^{-1})	12.29±4.69	11.15	6.10	24.30	38.2	10.35±4.10	9.30	8.10	24.20	39.6	9.09±2.21	8.90	8.10	16.20	24.3
Cl^{-} (mg l^{-1})	127.84±45.01	119.78	73.57	234.97	35.2	115.53±31.42	110.98	76.98	197.98	27.2	101.99±32.12	97.98	40.99	179.98	31.5
HCO_3^{-} (mg l^{-1})	13.87±3.77	13.33	6.67	20.00	27.2	13.33±5.77	13.33	0.00	23.33	43.3	12.00±5.53	11.67	0.00	20.00	46.1
SO_4^{2-} (mg l^{-1})	123.53±20.25	122.47	99.62	166.63	16.4	57.14±25.33	52.18	20.36	100.32	44.3	23.38±9.05	21.29	10.22	39.61	38.7
CO_3^{2-} (mg l^{-1})	0.00±0.00	0.00	0.00	0.00	-	0.00±0.00	0.00	0.00	0.00	-	0.00±0.00	0.00	0.00	0.00	-
Na^{+} (mg l^{-1})	105.18±25.87	102.00	73.00	165.00	24.6	66.48±5.54	66.00	54.00	75.00	8.3	45.56±18.75	42.00	10.00	74.00	41.2
K^{+} (mg l^{-1})	3.62±4.20	2.00	0.00	27.00	116.0	1.92±1.41	1.50	1.00	7.00	73.4	2.08±0.91	2.00	1.00	4.00	43.8

[Note: Ionic concentrations in mg l^{-1} except where specified]

Table. 4 PCA Loadings (Key Variables)

Parameter	PC1	PC2	PC3
pH	-0.08	-0.29	-0.05
EC	**0.40**	-0.31	0.36
TDS	**0.40**	-0.31	0.36
Ca^{2+}	0.35	0.13	-0.21
Mg^{2+}	0.28	0.03	**0.39**
Na^{+}	**0.35**	**0.39**	-0.32
Cl^{-}	**0.41**	0.34	-0.19
SO_4^{2-}	0.37	-0.16	-0.20
HCO_3^{-}	0.03	**0.57**	**0.45**
K^{+}	0.21	-0.30	-0.40

Table. 5 Eigenvalues and variance explained

Component	Variance Explained (%)	Cumulative (%)
PC1	**40.18 %**	40.18
PC2	**14.58 %**	54.76
PC3	**11.54 %**	66.30
PC4	10.11 %	76.41
PC5	7.85 %	84.26

Table. 6 Descriptive summary for hydrochemical Indices

	Core Zone			Mid Zone			Outer Zone		
Indices	**Mean ± SD**	**Min**	**Max**	**Mean ± SD**	**Min**	**Max**	**Mean ± SD**	**Min**	**Max**
Cl/Na Ratio	0.78±0.14	0.54	1.22	1.13±0.27	0.68	1.83	1.62±0.54	1.16	3.30
MH	45.42±13.58	16.69	66.71	44.13±7.59	33.38	59.95	48.85±3.50	33.38	52.78
PI	74.03±7.34	58.89	89.29	69.95±8.94	53.26	83.69	66.26±13.92	23.29	78.74
KR	2.15±0.74	1.14	5.06	1.62±0.49	0.92	2.45	1.32±0.56	0.30	2.25
RSC	-2.08±0.85	-4.39	-1.00	-1.73±0.67	-3.22	-0.95	-1.34±0.39	-2.45	-1.00
BEX	2.01±0.56	0.31	3.12	0.48±0.61	-0.76	1.69	-0.15±0.28	-0.61	0.29
CI	55.07±6.84	44.16	70.75	69.31±10.61	51.07	90.47	79.83±6.89	61.12	88.80
SAR	4.37±1.05	2.93	8.26	3.03±0.51	2.36	3.99	2.27±0.92	0.51	3.67

Table. 7 Statistical tests for hydrochemical indices

International Journal of Engineering Research & Technology (IJERT)
ISSN: 2278-0181
Vol. 15 Issue 06 , June - 2026

Index	Test	Test Statistic	df	p-value	Effect Size
Cl/Na Ratio	Kruskal-Wallis	H = 47.2	2	<0.001***	$\varepsilon^2 = 0.463$
BEX	Kruskal-Wallis	H = 72.8	2	<0.001***	$\varepsilon^2 = 0.721$
Chlorinity Index	Kruskal-Wallis	H = 51.3	2	<0.001***	$\varepsilon^2 = 0.504$
Kelly's Ratio	One-way ANOVA	F = 28.3	2, 97	<0.001***	$\eta^2 = 0.368$
MH	One-way ANOVA	F = 2.8	2, 97	0.065	$\eta^2 = 0.055$
PI	One-way ANOVA	F = 8.9	2, 97	<0.001***	$\eta^2 = 0.155$
RSC	Kruskal-Wallis	H = 18.7	2	<0.001***	$\varepsilon^2 = 0.176$
SAR	Kruskal-Wallis	H=61.30	2	<0.0001	$\varepsilon^2 = 0.619$

Table. 8 Irrigation suitability

Zone	MH Suitable	PI Suitable	RSC Suitable	KR Suitable	Overall Suitable
Core	96%	94%	100%	0%	0% (0/50)
Mid	96%	92%	100%	0%	0% (0/25)
Outer	96%	92%	100%	0%	0% (0/25)

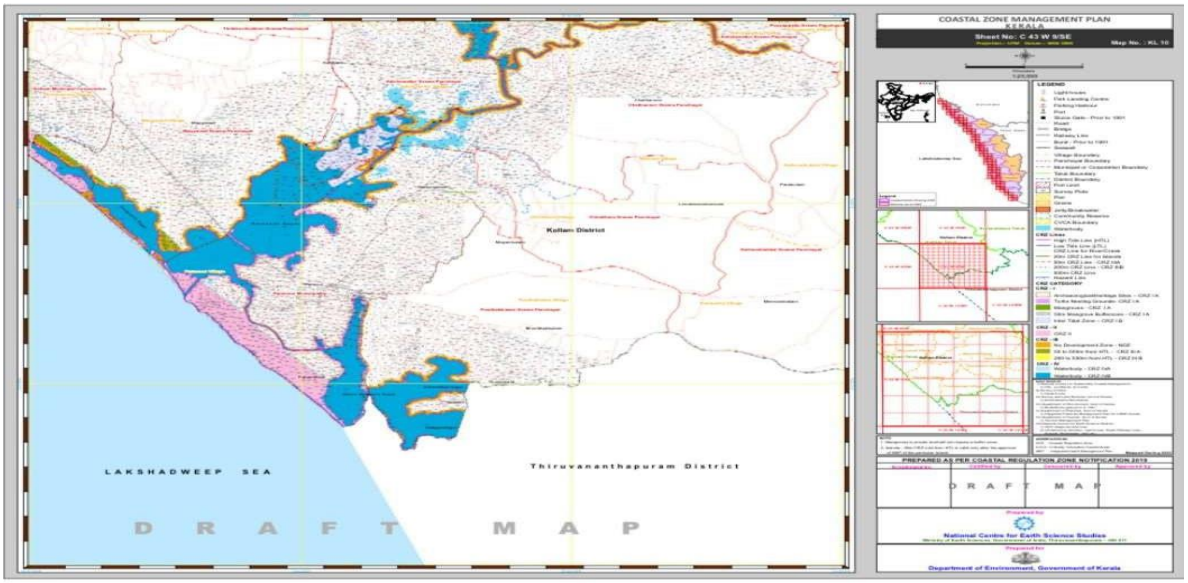

Fig. 1 Study Area - Paravur Municipality

International Journal of Engineering Research & Technology (IJERT)
ISSN: 2278-0181
Vol. 15 Issue 06 , June - 2026

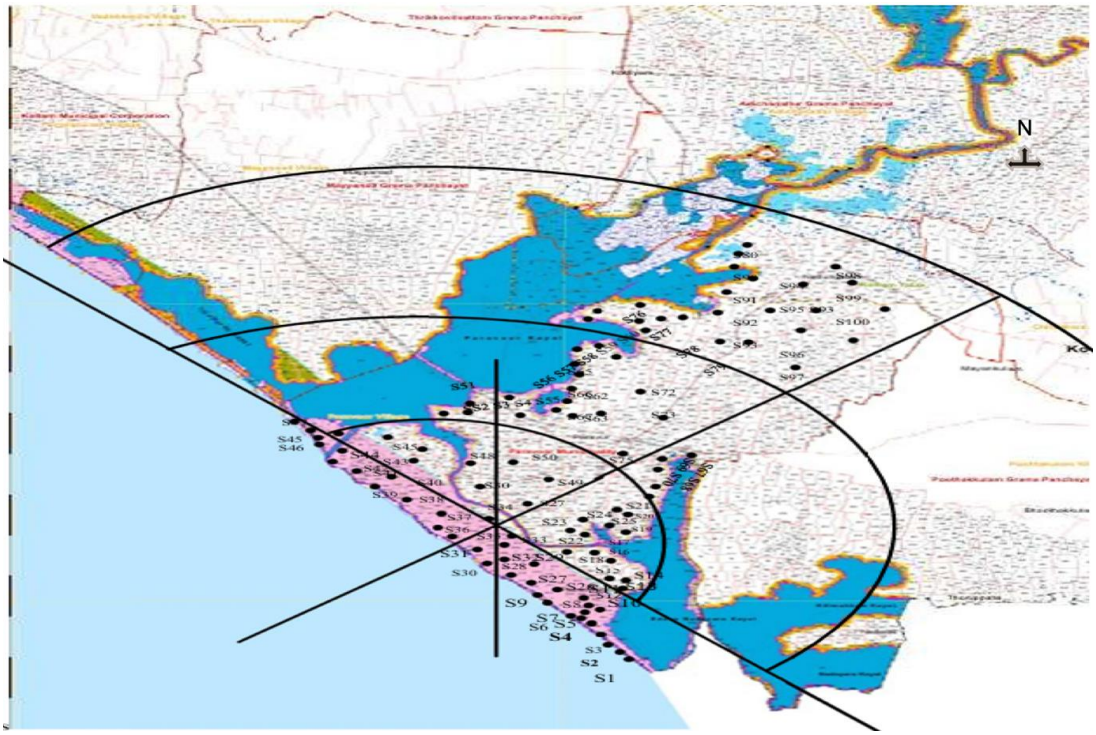

Fig. 2 Map of the study area showing the stratified sampling zones and sample distribution.

International Journal of Engineering Research & Technology (IJERT)
ISSN: 2278-0181
Vol. 15 Issue 06 , June - 2026

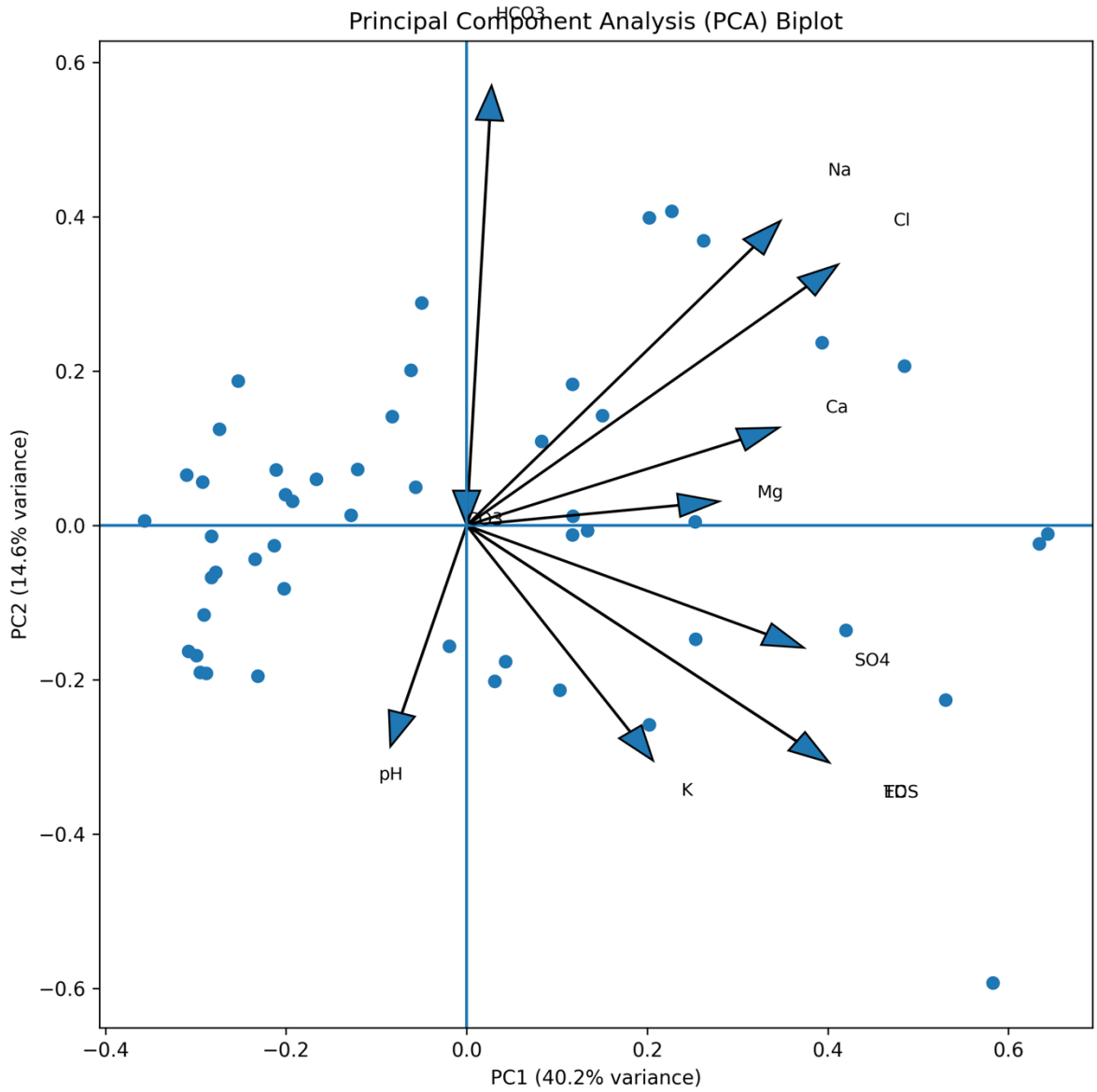

Fig. 3 Principal component analysis (PCA) biplot.

International Journal of Engineering Research & Technology (IJERT)
ISSN: 2278-0181
Vol. 15 Issue 06 , June - 2026

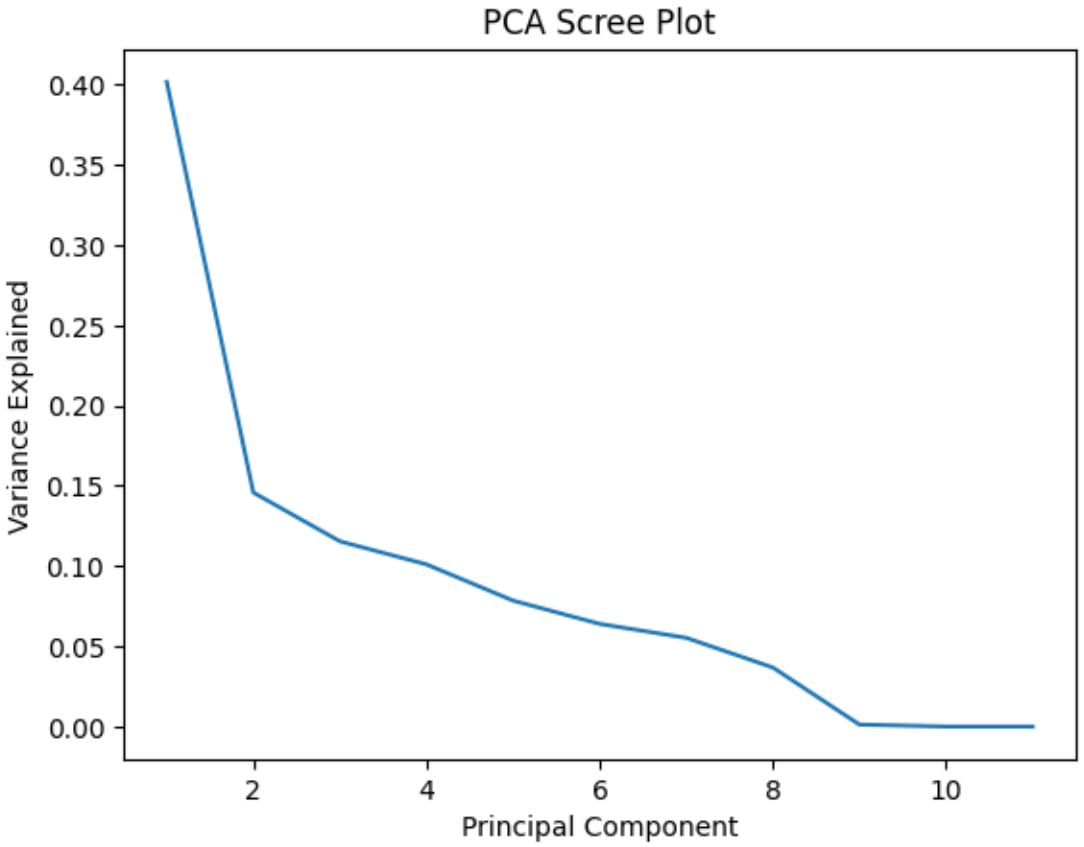

Fig. 4 PCA - Scree plot

Supplementary Materials - Irrigation Water Quality

Table S1: Sampling Design Decision Matrix

Criterion	Core Zone	Mid Zone	Outer Zone	Allocation Basis
Distance from coast	0-3 km	3-6 km	6-8.7 km	Zone definition
Approximate area	~8.1 km² (50%)	~4.9 km² (30%)	~3.2 km² (20%)	GIS analysis
Seawater entry points	3 (lake, sea, river)	1 (groundwater flow)	0 (distant)	Risk assessment
Estimated well count	~4,800 (60%)	~2,400 (30%)	~800 (10%)	Municipal records
Spatial heterogeneity	High (mixing zones)	Moderate (transition)	Low (uniform)	Literature review
Statistical minimum	n≥25	n≥25	n≥25	Power analysis
Area-proportional allocation	50	30	20	100 samples × area%
Risk-weighted allocation	75	20	5	High risk emphasis
Final allocation	**50**	**25**	**25**	**Balanced compromise**

Caption: Multi-criteria framework for stratified sample allocation. Final distribution (50:25:25) balances area representation, intrusion risk, well density, and statistical power requirements. Core Zone allocation (50) represents a compromise between area-proportional (50) and risk-weighted (75) approaches while ensuring adequate inland representation for detecting non-conventional intrusion patterns.

Table S2: Shapiro-Wilk Normality Test Results by Zone

Parameter	Core Zone (n=50)	Mid Zone (n=25)	Outer Zone (n=25)	Combined (n=100)
	W / p-value	W / p-value	W / p-value	W / p-value
pH	0.968 / 0.189	0.954 / 0.304	0.971 / 0.677	0.912 / <0.001***
EC	0.921 / 0.003**	0.972 / 0.687	0.953 / 0.282	0.931 / <0.001***

International Journal of Engineering Research & Technology (IJERT)
ISSN: 2278-0181
Vol. 15 Issue 06 , June - 2026

TDS	0.920 / 0.002**	0.971 / 0.672	0.951 / 0.259	0.929 / <0.001***
Cl^-	0.961 / 0.092	0.963 / 0.475	0.946 / 0.200	0.954 / 0.002**
Na^+	0.934 / 0.009**	0.962 / 0.454	0.881 / 0.008**	0.941 / <0.001***
SO_4^{2-}	0.917 / 0.002**	0.964 / 0.495	0.955 / 0.315	0.887 / <0.001***
Ca^{2+}	0.949 / 0.031*	0.948 / 0.226	0.971 / 0.678	0.973 / 0.042*
Mg^{2+}	0.975 / 0.368	0.961 / 0.432	0.979 / 0.873	0.981 / 0.186

*p < 0.05; **p < 0.01; ***p < 0.001

Table S3: Mean-Median Comparison and Distribution Characteristics

Parameter	**Core Zone**		**Mid Zone**		**Outer Zone**	
	Mean / Median Ratio	**Distribution**	**Mean / Median Ratio**	**Distribution**	**Mean / Median Ratio**	**Distribution**
pH	0.99	Symmetric	1.00	Symmetric	0.99	Symmetric
EC	1.07	Right-skewed	1.01	Symmetric	1.05	Right-skewed
TDS	1.07	Right-skewed	1.03	Symmetric	1.08	Right-skewed
Ca^{2+}	1.12	Right-skewed	1.10	Right-skewed	1.06	Right-skewed
Mg^{2+}	1.10	Right-skewed	1.11	Right-skewed	1.02	Symmetric
Cl^-	1.07	Right-skewed	1.04	Symmetric	1.04	Symmetric
Na^+	1.03	Symmetric	1.01	Symmetric	1.08	Right-skewed
K^+	1.81	Highly right-skewed	1.28	Right-skewed	1.04	Symmetric

[Interpretation Guide: Ratio ≈ 1.0: Symmetric distribution; Ratio > 1.1: Right-skewed (presence of high outliers); Ratio < 0.9: Left-skewed (presence of low outliers)]

Table S4: Correlation Matrix (Pearson's r) with Principal Components

	PC1	PC2	Cl/Na	KR	BEX	CI	MH	PI	RSC
PC1	1.00								
PC2	-0.08	1.00							
Cl/Na	0.71**	-0.35*	1.00						
KR	0.42**	-0.58**	0.28*	1.00					
BEX	-0.31*	0.92**	-0.42**	-0.64**	1.00				
CI	0.84**	-0.22	0.69**	0.31*	-0.28*	1.00			
MH	-0.18	0.14	-0.08	-0.21	0.16	-0.12	1.00		
PI	-0.53**	0.38*	-0.44**	-0.67**	0.51**	-0.48**	0.22	1.00	
RSC	0.36*	0.45**	0.19	-0.72**	0.58**	0.24	0.31*	0.74**	1.00

[Note: *p < 0.05, **p < 0.001]